

Microscopic 8-quark study of the antikaon nucleon nucleon systems

P. Bicudo

CFTP, Dep. Física, Instituto Superior Técnico, Av. Rovisco Pais, 1049-001 Lisboa, Portugal

We study the possibility to bind eight quarks in a molecular hadronic system composed of two nucleons and an antikaon, with the quantum numbers of a hexaquark flavour, in particular with strangeness -1, isospin 1/2, parity -, baryonic number 2 and two possible spins, 0 or 1. These exotic hadrons are motivated by the deuteron, a proton-neutron boundstate, and by the model of the $\Lambda(1405)$ as an anti-kaon proton boundstate. We discuss the possible production of this hadron in the experiments which are presently investigating hot topics like the Θ^+ pentaquark or the K^- deeply bound in nuclei. The $K^- \bullet N$ interactions and the coupling to other channels are computed microscopically from a confining and chiral invariant quark model resulting in local plus separable Gaussian potentials. The $N \bullet N$ interactions used here are the state of the art Nijmegen potentials. The binding energy and the decay rate of the $K^- \bullet N$ and $K^- \bullet N \bullet N$ systems are computed with configuration space variational methods. The only system that binds with our microscopic interaction is the $K^- \bullet N$ in the $I = 0$ channel, compatible with the $\Lambda(1405)$.

I. INTRODUCTION

Here we study the binding energy of a possible molecular antikaon, nucleon and nucleon three-body system. Importantly, from a hadronic perspective, a bound $K^- \bullet N \bullet N$ can be at most reduced to a hexaquark, a exotic system. In a nuclear perspective, the deep binding of antikaons in nuclei has been predicted and are also actively searched. A bound $K^- \bullet N \bullet N$ would constitute a simple antikaon-nucleus system, the ${}^2_{K^-}H$.

Moreover, the $K^- \bullet N \bullet N$ can be formed with anti-Kaon (K^-) deuteron ($p \bullet n$) scattering. Other exotic tetraquarks, pentaquarks or hexaquarks are also very plausible, but they are all harder to produce experimentally because they would need at least strangeness and charm. The several experiments dedicated to pentaquark searches (where not only the kaon, but also the antikaon may interact with nuclei), or to antikaon-nuclear binding at RCNP, JLab, KEK, DAFNE and at many other laboratories, are already able to search for the proposed $K^- \bullet N \bullet N$. In particular evidence for $K^- \bullet N \bullet N$ has already been found by the FINUDA collaboration at DAFNE [2, 3]. In Fig. 1 different possible production mechanisms are depicted. They are similar to the $\Lambda(1405)$ production mechanisms, except that the K^- scatters on a deuterium nucleus, not on a hydrogen nucleus. The process in Fig. 1 (a) is only possible if the width of the $K^- \bullet N \bullet N$ is of the order of its binding energy. The process in Fig. 1 (b) is always possible, but is suppressed by the electromagnetic coupling. Processes in Fig. 1 (c), (d) are dominant. The production process (c) should occur in experiments designed for the production of the pentaquark Θ^+ , where the K^- has sufficient energy to create a π . The production process (d) should occur in atomic kaon experiments, where the K^- has a low energy but where a larger nucleus is used and the remaining nucleus may absorb the virtual pion.

The $K^- \bullet N \bullet N$ binding is suggested by the deuteron 2H , a proton-neutron boundstate, and by the model of the $\Lambda(1405)$ as an anti-kaon proton boundstate. How-

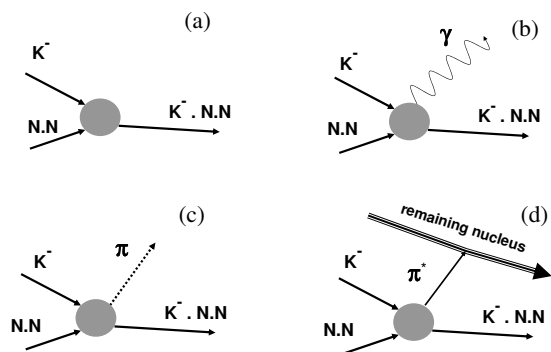


FIG. 1: Different $K^- \bullet N \bullet N$ production mechanisms .

ever the subtleties of these two-body subsystems require a precise computation of the binding energy of the three-body system. For instance the binding of the deuteron ($p \bullet n$) requires a d-wave component [4]. Moreover it is not clear yet if the $K^- \bullet N$ binds in an $I = 1 \Sigma$ baryon. Notice that in the $I = 0$ channel there is strong evidence that the $\Lambda(1405)$ is constituted of two poles, respectively dominated by the $K^- \bullet N$ and the $\pi \bullet \Sigma$ channels [6, 7, 8, 9, 10, 11, 12, 13].

The $K^- \bullet N \bullet N$ binding is a very recent topic. While Oset, Toki and collaborators [14, 15] offer a different interpretation to the FINUDA peak, very recent theoretical calculations, fitting the $K^- \bullet N$ scattering data with effective local potentials [16, 17, 18] or with separable potentials [19] agree with a relatively deep and wide $K^- \bullet N \bullet N$ resonance.

Here we specialize in the microscopic quark computation of the binding energy and width of the $K^- \bullet N \bullet N$ systems. Section II is dedicated to the $N \bullet N$ and $K \bullet N$ interactions. We compute microscopically the $K \bullet N$ interaction, with a confining and chiral invariant quark model and using the Resonating Group Method. In Section III we calibrate our interactions with the experimental $K^+ \bullet N$ data, and we study the binding and decay of $K^- \bullet N$ and $K^- \bullet N \bullet N$ systems. Finally we conclude.

II. FROM QUARKS TO THE $K \bullet N$

There are several very precise models of the $N \bullet N$ interaction [4], compatible with the experimental $N \bullet N$ phase shifts. All contain a long-range attractive potential, a medium-range attractive potential, an a hard core or short range potential. A picture consistent with QCD emerges if the long range attraction is due to the Yukawa one-pion-exchange, the medium range is due to two-pion or one-sigma exchange, while the short range repulsion is dominated by the quark interactions. Different models exist because the ${}^3S_1 \leftrightarrow {}^3D_1$ coupling is partly equivalent to the attractive part of the 3S_1 potential. Moreover the repulsive hard core potential essentially pushes the wavefunction outside the repulsive core region, and this can be accomplished for different heights of the repulsive core. Also, separable or local potentials can be used.

However the $K^- \bullet N$ interaction has not yet been modelled with the same detail of the $N \bullet N$ interaction [5]. Notice that not only the kaons are unstable particles, with less experimental results, but also there are large inelastic coupled channel effects in the $K^- \bullet N$ scattering. Moreover, there is strong evidence that the $\Lambda(1405)$ does not have a single pole with width Γ of $40MeV$, but two narrower poles, one closer to the $K^- \bullet N$ threshold and another dominated by the $\pi \bullet \Sigma$ channel.

This leads us to compute the $K^- \bullet N$ interaction microscopically at the quark level. Here we assume a standard Quark Model (QM) Hamiltonian,

$$H = \sum_i T_i + \sum_{i < j, \vec{i} < \vec{j}} V_{ij} + \sum_{i, \vec{j}} A_{i\vec{j}}, \quad (1)$$

where each quark or antiquark has a kinetic energy T_i with a constituent quark mass, and the colour dependent two-body interaction V_{ij} includes the standard QM confining term and a hyperfine term,

$$V_{ij} = \frac{-3}{16} \vec{\lambda}_i \cdot \vec{\lambda}_j \left[V_{conf}(r) + V_{hyp}(r) \vec{S}_i \cdot \vec{S}_j \right]. \quad (2)$$

For the purpose of this paper the details of potential (2) are unimportant, we only need to estimate its matrix elements. The hadron spectrum is compatible with,

$$\langle V_{hyp} \rangle \simeq \frac{4}{3} (M_\Delta - M_N) \quad (3)$$

Moreover we include in the Hamiltonian (1) a quark-antiquark annihilation potential $A_{i\vec{j}}$. Notice that the quark-antiquark annihilation is constrained when the quark model produces spontaneous chiral symmetry breaking [20, 21, 22, 23, 24, 25]. In the π Salpeter equation, the annihilation potential A cancels most of the kinetic energy and confining potential $2T + V$,

$$\langle A \rangle_{S=0} \simeq \langle 2T + V \rangle_{S=0} \simeq \langle V_{hyp} \rangle, \quad (4)$$

leading to a massless pion in the chiral limit. We stress that the QM of eq. (1) not only reproduces the meson

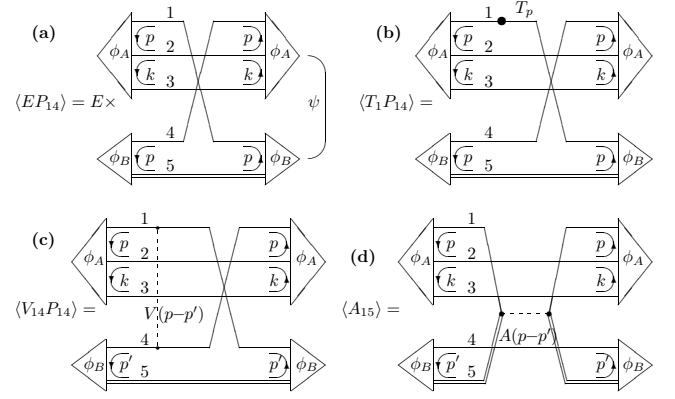


FIG. 2: Examples of our RGM overlaps for the baryon-meson effective interaction: (a) norm exchange overlap; (b) kinetic exchange overlap; (c) interaction exchange overlap; (d) annihilation overlap.

and baryon spectra as quark and antiquark bound-states, but it also complies with the PCAC theorems [23, 24, 25, 26, 27].

For the pentaquark system, the Resonating Group Method(RGM) [28] is convenient to arrange the wave functions of quarks and antiquarks in antisymmetrized overlaps of simple colour singlet quark clusters, the baryons and mesons. The effective potential of the meson-baryon system is computed with the overlap of the inter-cluster microscopic potentials,

$$V_{mes B}^{\text{bar } A} = \langle \phi_B \phi_A | - (V_{14} + V_{1\bar{5}} + 2V_{24} + 2V_{2\bar{5}}) 3P_{14} + 3A_{1\bar{5}} | \phi_A \phi_B \rangle / \langle \phi_B \phi_A | 1 - 3P_{14} | \phi_A \phi_B \rangle, \quad (5)$$

where P_{ij} stands for the exchange of particle i with particle j , see Fig. 2. This results in an algebraic colour \times spin \times flavour factor and a spatial overlap. A convenient basis for the spatial wave-functions of the meson A and the baryon B is the harmonic oscillator basis,

$$\phi_{000}^\alpha(\rho) = \mathcal{N}_\alpha^{-1} \exp\left(-\frac{\rho^2}{2\alpha^2}\right), \quad \mathcal{N}_\alpha = (\sqrt{\pi}\alpha)^{\frac{3}{2}}. \quad (6)$$

In what concerns the quark exchange diagrams, the spin independent part of the quark-quark(antiquark) potential in eq. (2) essentially vanishes because the clusters are colour singlets. The only potential which may contribute is the hyperfine potential. The quark Pauli exchange also leads to a positive, repulsive potential.

Importantly, each annihilation diagram can be related to an exchange diagram with the crossing symmetry of one of incoming baryon with the outgoing baryon. This is evident in Fig. 2 (c) and Fig. 2 (d). The corresponding diagrams are opposite because the annihilation diagram does not have the Pauli exchange minus sign of the exchange diagram. Another important difference occurs, the exchange diagrams produce non-local simple separable potentials, while the annihilation diagrams produce simple local Gaussian potentials. Nevertheless all the

different diagrams produce hard core potentials proportional to $\langle V_{hyp} \rangle$, repulsive in exchange diagrams and attractive in annihilation diagrams. Notice that attraction may only occur in non-exotic channels.

We summarize [29, 30, 31, 32, 33] the effective potentials computed for the relevant channels,

$$\begin{aligned} V_{K \bullet N} &= c_K^2 \langle V_{hyp} \rangle \frac{23}{32} \left(1 + \frac{20}{23} \vec{\tau}_K \cdot \vec{\tau}_N \right) |\phi_{000}^\alpha \rangle \langle \phi_{000}^\alpha|, \\ V_{\bar{K} \bullet N}(\mathbf{r}) &= -c_K^2 \langle V_{hyp} \rangle 2\sqrt{2} \left(1 - \frac{4}{3} \vec{\tau}_K \cdot \vec{\tau}_N \right) e^{-r^2/\alpha^2}, \\ V_{\bar{K} \bullet N \leftrightarrow \pi \bullet \Lambda} &= c_\pi c_K \langle V_{hyp} \rangle \frac{9}{32} \left(1 + \frac{4}{3} \vec{\tau}_K \cdot \vec{\tau}_N \right) |\phi_{000}^\alpha \rangle \langle \phi_{000}^\alpha|, \\ V_{\bar{K} \bullet N \leftrightarrow \pi \bullet \Sigma} &= c_\pi c_K \langle V_{hyp} \rangle \frac{-5}{8} \left(\frac{1+\sqrt{6}}{4} + \frac{-3+\sqrt{6}}{3} \vec{\tau}_K \cdot \vec{\tau}_N \right) |\phi_{000}^\alpha \rangle \langle \phi_{000}^\alpha|, \end{aligned} \quad (7)$$

where $\vec{\tau}$ are 1/2 of the Pauli isospin matrices for the $I = 0$ and $I = 1$ cases, and $c_\pi = \sqrt{E_\pi} f_\pi (\sqrt{2\pi}\alpha)^{3/2} / \sqrt{3}$ is a PCAC factor, and \mathbf{r} is the relative coordinate.

We calibrate our parameters in the two-body $K \bullet N$ channels, where the diagonalization of the finite difference hamiltonian is straightforward. From baryon spectroscopy we get $\langle V_{hyp} \rangle = 390 \text{ MeV}$. Since c_K is a PCAC factor that suppresses the norm of quasi-Golstonebosons, consistent with the Adler zero in the chiral limit, we get the plausible parameter interval $c_K^2 \langle V_{hyp} \rangle \in [200, 300] \text{ MeV}$. From the phase shifts for the first channel of eq. (7), the repulsive and well understood $S = 1$ $K \bullet N$ channel [34, 35, 36] depicted in Fig. 3, we determine the size parameter $\alpha \in [0.34, 0.39] \text{ fm}$. This is necessarily smaller, by a factor of 2, than the hadronic charge radius which is enhanced by the vector meson dominance.

III. RESULTS AND CONCLUSION

To study the binding and decay of the $K^- \bullet N$ two-body systems and of the $K^- \bullet N \bullet N$ three-body systems, we diagonalize the hamiltonian in configuration space. Importantly, the decay widths to the channels $\pi \bullet \Sigma$ and $\pi \bullet \Sigma \bullet N$ are accounted with the substitution method, resulting in an effective two-body $K^- \bullet N$ separable potential $-|\phi_{000} \rangle \langle \phi_{000}| G_0(E) |\phi_{000} \rangle \langle \phi_{000}|$. Because the energy E of our plausible resonances is above the pionic channels, the Green function matrix elements are complex. This produces the decay width contribution $-i\Gamma/2$ to the eigenvalues of the Schrödinger two-body and three-body Hamiltonians.

First we study the Λ channel with the $I = 0$ two-body $K^- \bullet N$ system. Using the PCAC ratio $c_\pi/c_K = \sqrt{E_\pi/M_K} \simeq 0.56$, and solving the $K^- \bullet N$ Schrödinger equation in this parameter range, including the coupling to the $\pi \bullet \Sigma$ effective potential, we get a resonance in the $\Lambda(1405)$ region, with binding energy $M - m_K - m_N \in [-23.8, -1.7] \text{ MeV}$, and width $\Gamma \in [3.5, 7.0] \text{ MeV}$. This is distant from the single Breit-Wigner model for the $\Lambda(1405)$ resonance, with a width of $\Gamma \simeq 40 \text{ MeV}$ [37] and a binding energy of -30 MeV . We also consider an increase of the chiral coupling up to $c_\pi/c_K = 1$,

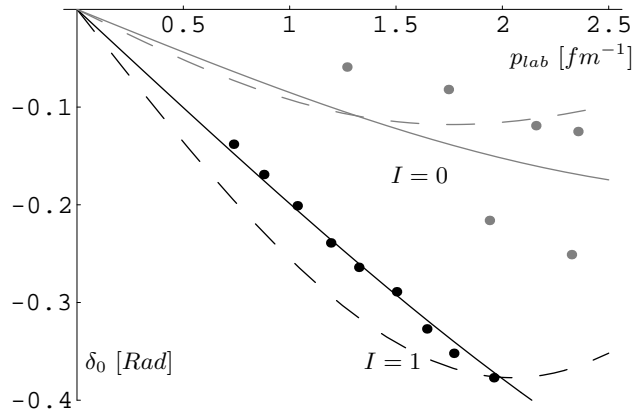


FIG. 3: $I = 0$ (grey) and $I = 1$ (black) s-wave $K \bullet N$ phase shifts as a function of the kaon momentum in the laboratory frame. The dots are experimental [34, 35, 36] and the solid lines represent this model [29, 30, 31, 32, 33] with the hadronic size parameter $\alpha = 0.36 \text{ fm}$ and $c_K^2 V_{hyp} = 436/\sqrt{8} = 250 \text{ MeV}$. A much larger $\alpha = 0.66 \text{ fm}$, even with a small $c_K^2 V_{hyp} = 45 \text{ MeV}$ potential strength, would produce a worse fit (dashed line).

to simulate the possible effect of other decay channels. Maintaining the remaining parameter ranges, the resonance approaches the $\Lambda(1405)$ region, with binding energy $M - m_K - m_N \in [-42.2, -7.7] \text{ MeV}$, and width $\Gamma \in [11.2, 23.0] \text{ MeV}$. This is reasonably close to the $\Lambda(1405)$, possibly also close to its double pole models, including a slightly narrower Breit-Wigner pole closely below the $K^- \bullet N$ threshold (here we don't address the second pole, since for simplicity we did not include the $\pi \bullet \Sigma$ interaction, less relevant for the $K^- \bullet N \bullet N$ system).

It is then instructive to find how much we can decrease the $I = 0$ attraction, and still bind the $K^- \bullet N$ system. Excluding the coupled channels, the $V_{K^- \bullet N}$ attraction is marginally sufficient to bind the $I = 0$ system, up to a 1 MeV binding energy. The coupled channel effects further bind the system and, even if the overall $I = 0$ attraction is reduced by a factor $\in [0.77, 0.89]$, binding occurs.

In the Σ channel with the $I = 1$ two-body $K^- \bullet N$ system, according to eq. (7), the $V_{K^- \bullet N}$ attraction is decreased by a factor of $\frac{1}{3}$, when compared with the $I = 0$ channel. Clearly, this small potential is far from being able to bind the $K^- \bullet N$ onto a Σ .

We finally study the $K^- \bullet N \bullet N$ three-body system, using the Nijmegen REID93 potential [4], together with our $K^- \bullet N$ interaction and our coupling to the $\pi \bullet \Sigma$ and $\pi \bullet \Lambda$ channels. Importantly, our two-body sub-systems only bind for isospin $I = 0$. For the $N \bullet N$ sub-system we can either have isospin $I_{NN} = 0$ and spin $S_{NN} = 1$, or $I_{NN} = 1$ and $S_{NN} = 0$. The two different total $I = \frac{1}{2}$ systems are respectively the $(-K^- pn + K^- np)/\sqrt{2}$ with spin 1, and the $(2\bar{K}_0 nn - K^- pn - K^- np)/\sqrt{6}$ with spin 0. In the $S = 1$ case, each $K^- \bullet N$ sub-system is $\frac{1}{4}$ in a Λ -like $I = 0$ state and $\frac{3}{4}$ in a Σ -like $I = 1$ state. In the $S = 0$

case, each $K^- \bullet N$ sub-system is $\frac{5}{12}$ in a Λ -like $I = 0$ state and $\frac{7}{12}$ in a Σ -like $I = 1$ state. Let us now consider the case where the two nucleons would be superposed, and use eq. (7) to estimate the attraction that this dinucleon would impose on the anti-kaon. In the $S = 1$ system, the K^- would feel an attraction identical to the one it feels in the Λ system. In the $S = 0$ system, the K^- would feel an attraction slightly larger, by a factor of $\frac{11}{9}$. Qualitatively, because our K^- binds only marginally to the N in the Λ system, binding is unlikely in the $S = 0$ three-body system, where the $N \bullet N$ is unbound. The $S = 1$ three-body system is more likely to bind because it includes a deuteron.

Nevertheless a quantitative study is necessary because the nucleons are strongly repelled at short distance, and their separation weakens the attraction of the anti-kaon. It is then convenient to replace the coordinates of the three hadrons N_1 , N_2 and K^-_3 by relative and centre of mass coordinates

$$\begin{pmatrix} \mathbf{r}_{12} \\ \mathbf{r}_{123} \\ \mathbf{R} \end{pmatrix} = \begin{pmatrix} 1 & -1 & 0 \\ \frac{1}{2} & \frac{1}{2} & -1 \\ \frac{\gamma}{2+\gamma} & \frac{\gamma}{2+\gamma} & \frac{\gamma}{2+\gamma} \end{pmatrix} \begin{pmatrix} \mathbf{r}_{N1} \\ \mathbf{r}_{N2} \\ \mathbf{r}_{K3} \end{pmatrix} \quad (8)$$

where $\gamma = m_K/m_N$. The coordinate \mathbf{R} is eliminated in the centre of mass frame, and we rewrite the hamiltonian in terms of scalar products of \mathbf{r}_{12} , \mathbf{r}_{123} and their momenta \mathbf{p}_{12} and \mathbf{p}_{123} . The total kinetic energy,

$$T = \frac{1}{2} \frac{2}{m_N} \mathbf{p}_{12}^2 + \frac{1}{2} \frac{2+\gamma}{2\gamma m_N} \mathbf{p}_{123}^2, \quad (9)$$

is diagonal in \mathbf{p}_{12} and \mathbf{p}_{123} . The $V_{N_1 N_2}$ potential only depends on \mathbf{r}_{12} , including the tensor interaction. The sum of the other potentials $V_{N_1 K_3} + V_{N_2 K_3}$ is a function of r_{12} , r_{123} and of the square of $\omega = \hat{r}_{12} \cdot \hat{r}_{123}$. To span the possible quantum numbers of $K^- \bullet N \bullet N$ system, we apply the total potential energy to a groundstate product of s-wave wavefunctions of \mathbf{r}_{12} and of \mathbf{r}_{123} . In what concerns the angular quantum numbers, the tensor part of the $N \bullet N$ interaction $V_{N_1 N_2}$ will couple the s-wave in \mathbf{r}_{12} to a d-wave. The other two potentials $V_{N_1 K_3} + V_{N_2 K_3}$ couple the groundstate s-wave product to wave-functions with any even power of ω . We address the binding of the three-body $K^- \bullet N \bullet N$ system with two different applications of the variational method. In the first method, we use a basis of Laguerre Polynomials in the radial variables r_{12} and r_{123} ,

$$\nu_{nl}^\alpha(r) = \sqrt{\frac{2^{3+2l} n!}{(n+2+2l)!}} \frac{r^{1+l}}{\alpha^{3/2+l}} e^{-r/\alpha} L_n^{2+2l} \left(\frac{r}{\alpha} \right), \quad (10)$$

adequate to study weakly bound systems, together with a basis of Legendre polynomials $P_l(\omega)$ in the angular variable ω . We use up to 10 excitations in each Laguerre basis and 5 excitations in the Legendre basis, sufficient to get for instance the deuteron binding. In the second method we use a finite difference method, with 40 excitations in each of the radial variables, and 3 in the angular

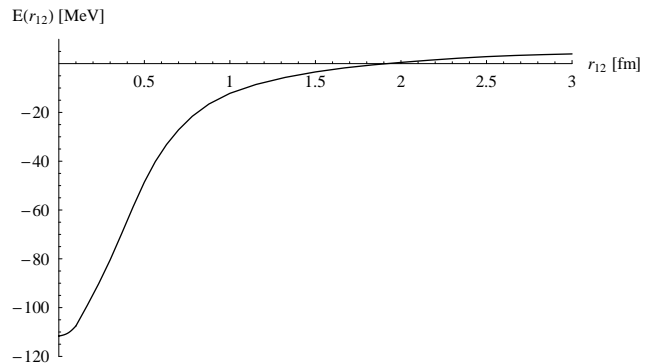


FIG. 4: Kaon energy, or real part of the lowest s-wave eigenvalue of $T_{123} + T_w + V_{N_1 K_3} + V_{N_2 K_3}$, as a function of the nucleon-nucleon distance $r_{12} = |r_{N_1} - r_{N_2}|$. This result is obtained in a large sphere with a r_{123} radius of 7.5 fm. In the infinite sphere radius limit the energy essentially vanishes for $r_{12} > 2.0$ fm.

variable. The binding and decay width of the $K^- \bullet N \bullet N$ are determined from the lowest eigenvalue of the hamiltonian, both in the polynomial basis and in the finite difference basis.

It turns out that the $K^- \bullet N \bullet N$ systems do not bind. The most favourable case is the $I = 1/2$, $S = 1$ channel, where the groundstate has binding in the r_{12} coordinate, but no binding in the r_{123} coordinate. In particular, the r_{12} part of the wavefunction is localized and reproduces the deuteron wavefunction, while the r_{123} part is extended over the whole size of the large box where we quantize the wave-function. In the limit where the size of the box is infinite, we get a bound deuteron $p \bullet n$ and a free K^- .

To study in more detail how far we are from binding, we consider the adiabatic limit of the $I = 1/2$, $S = 1$ system, where the positions of the two nucleons are frozen, by fixing the r_{12} variable. Then the energy of the kaon K^- can be computed, diagonalizing in detail the terms in the hamiltonian depending on r_{123} and w . The resulting smaller eigenvalue of $T_{123} + T_w + V_{N_1 K_3} + V_{N_2 K_3}$ is shown in Fig. 4, using the parameters in our interval that provide the strongest possible binding. It occurs that the antikaon is bound to this frozen deuteron system only if $r_{12} < 2.0$ fm.

Notice that this is much smaller than the deuteron double radius mean square $\sqrt{\langle r_{12}^2 \rangle} = 3.9$ fm, which is quite large because at short distances the $N \bullet N$ subsystem suffers a strong repulsion and because the deuteron is weakly bound. Thus it would be very hard to contract the deuteron to a sufficiently small radius to bind the antikaon. Then, at these large distances, the antikaon essentially feels a double-well potential, as shown in Fig. 5. Importantly, such a widely separated double-well potential only binds if any of the two wells is sufficiently deep to bind the antikaon. It occurs that this already happens if the $K^- \bullet N$ attraction is arbitrarily increased by 16%. Assuming a sufficient arbitrary increase of the

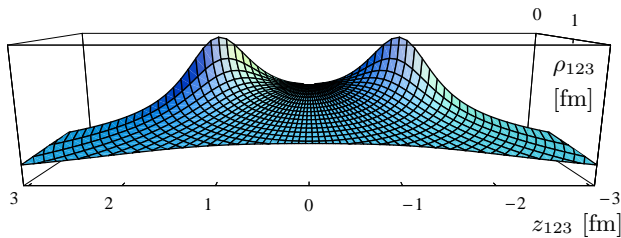


FIG. 5: 3d perspective (colour online) of the antikaon wavefunction, assuming two adiabatically frozen nucleons at the distance of $r_{12} = 2.5$ fm, obtained with polar coordinates for the \mathbf{r}_{123} , with finite differences, and with a radial lattice spacing of 0.1 fm. In this unbound case, the wavefunction is a deformation of the lowest positive energy harmonic.

interactions, then we estimate that at low binding energies $M - m_K - 2m_N \in [-10, -2]$ MeV, the decay width to the $\pi \bullet \Sigma \bullet N$ channel would be $\Gamma \in [7, 18]$ MeV, comparable to the double of the binding energy, but narrower than the $\Lambda(1405)$ width. This small width occurs because the antikaon wavefunction extends far from the nucleons.

To conclude we compute, starting at the quark level,

the $K^- \bullet N$ interactions, constrained by chiral symmetry and by the crossing symmetry to the $K^+ \bullet N$ system. We find binding in the $I = 0$, $K^- \bullet N$ channel, possibly consistent with the double pole model of the $\Lambda(1405)$, and no binding in the $I = 1$, $K^- \bullet N$ two-body Σ . In the $I = 1/2$, $S = 1$, $K^- \bullet N \bullet N$ and $S = 0$, $K^- \bullet N \bullet N$ three-body systems, we find no binding, although we almost get binding. Essentially, the main difference from our non-binding and from the significant binding and decay of very recent theoretical calculations [5, 16, 17, 18, 19] can be linked to our shorter range and weaker potential $V_{K^- N}$.

Since a small parameter change may lead to binding in the $K^- \bullet N \bullet N$ systems, and since ten-quark or twelve-quark components may affect the longer range part of the interaction, we recommend that the $K^- \bullet N \bullet N$ systems should continue to be explored, both experimentally and theoretically.

Acknowledgments

PB thanks Eulogio Oset and Paola Gianotti for discussions on the $K^- \bullet N \bullet N$ systems and Marco Cardoso and George Rupp for support on the $N \bullet N$ interaction.

-
- [1] P. Bicudo and G. M. Marques, Phys. Rev. D **69**, 011503(R) (2004) [arXiv:hep-ph/0308073].
- [2] M. Agnello *et al.* [FINUDA Collaboration], Phys. Rev. Lett. **94** (2005) 212303.
- [3] M. Agnello *et al.*, arXiv:nucl-ex/0606021.
- [4] V. G. J. Stoks, R. A. M. Klomp, C. P. F. Terheggen and J. J. de Swart, Phys. Rev. C **49**, 2950 (1994) [arXiv:nucl-th/9406039]; *online codes at* <http://nn-online.org>.
- [5] Y. Akaishi and T. Yamazaki, Phys. Rev. C **65**, 044005 (2002).
- [6] V. K. Magas, E. Oset and A. Ramos, Phys. Rev. Lett. **95**, 052301 (2005) [arXiv:hep-ph/0503043].
- [7] J. A. Oller and U. G. Meissner, Phys. Lett. B **500** (2001) 263 [arXiv:hep-ph/0011146].
- [8] D. Jido, A. Hosaka, J. C. Nacher, E. Oset and A. Ramos, Phys. Rev. C **66** (2002) 025203 [arXiv:hep-ph/0203248].
- [9] C. Garcia-Recio, J. Nieves, E. Ruiz-Arriola and M. J. Vicente-Vacas, Phys. Rev. D **67** (2003) 076009 [arXiv:hep-ph/0210311].
- [10] D. Jido, J. A. Oller, E. Oset, A. Ramos and U. G. Meissner, Nucl. Phys. A **725** (2003) 181 [arXiv:nucl-th/0303062].
- [11] C. Garcia-Recio, M. F. M. Lutz and J. Nieves, Phys. Lett. B **582** (2004) 49 [arXiv:nucl-th/0305100].
- [12] T. Hyodo, S. I. Nam, D. Jido and A. Hosaka, Phys. Rev. C **68** (2003) 018201 [arXiv:nucl-th/0212026].
- [13] S. I. Nam, H. C. Kim, T. Hyodo, D. Jido and A. Hosaka, arXiv:hep-ph/0309017.
- [14] E. Oset and H. Toki, Phys. Rev. C **74**, 015207 (2006) [arXiv:nucl-th/0509048].
- [15] V. K. Magas, E. Oset, A. Ramos and H. Toki, Phys. Rev. C **74**, 025206 (2006) [arXiv:nucl-th/0601013].
- [16] A. N. Ivanov, P. Kienle, J. Marton and E. Widmann, arXiv:nucl-th/0512037.
- [17] T. Yamazaki and Y. Akaishi, arXiv:nucl-ex/0609041.
- [18] T. Yamazaki and Y. Akaishi, arXiv:nucl-th/0604049.
- [19] N. V. Shevchenko, A. Gal and J. Mares, arXiv:nucl-th/0610022.
- [20] P. Bicudo and J. E. Ribeiro, Phys. Rev. D **42**, 1611 (1990); Phys. Rev. D **42**, 1625 (1990); Phys. Rev. D **42**, 1635 (1990).
- [21] P. Bicudo, Phys. Rev. C **60**, 035209 (1999).
- [22] F. J. Llanes-Estrada and S. R. Cotanch, Phys. Rev. Lett. **84**, 1102 (2000) [arXiv:hep-ph/9906359].
- [23] P. Bicudo, Phys. Rev. C **67**, 035201 (2003).
- [24] P. Bicudo, S. Cotanch, F. Llanes-Estrada, P. Maris, J. E. Ribeiro and A. Szczepaniak, Phys. Rev. D **65**, 076008 (2002) [arXiv:hep-ph/0112015].
- [25] P. Bicudo, M. Faria, G. M. Marques and J. E. Ribeiro, Nucl. Phys. A **735**, 138 (2004) [arXiv:nucl-th/0106071].
- [26] R. Delbourgo and M. D. Scadron, J. Phys. G **5**, 1621 (1979).
- [27] F. J. Llanes-Estrada and P. Bicudo, Phys. Rev. D **68**, 094014 (2003) [arXiv:hep-ph/0306146].
- [28] J. Wheeler, Phys. Rev. **52**, 1083 (1937); **52**, 1107 (1937).
- [29] P. Bicudo and J. E. Ribeiro, Z. Phys. C **38**, 453 (1988).
- [30] P. Bicudo, J. E. Ribeiro and J. Rodrigues, Phys. Rev. C **52**, 2144 (1995).
- [31] P. Bicudo, Nucl. Phys. A **748**, 537 (2005) [arXiv:hep-ph/0401106].
- [32] P. Bicudo, Phys. Rev. D **70**, 111504(R) (2004) [arXiv:hep-ph/0403146].
- [33] P. Bicudo, Phys. Rev. D **74**, 036008 (2006) [arXiv:hep-ph/0512041].
- [34] J. S. Hyslop, R. A. Arndt, L. D. Roper and R. L. Workman, Phys. Rev. D **46** 961 (1992).
- [35] T. Barnes and E. Swanson, Phys. Rev. C **49** 1166 (1994);
- [36] R. A. Arndt, I. I. Strakovsky and R. L. Workman,

Int. J. Mod. Phys. A **18**, 449 (2003); *online codes at*
<http://gwdac.phys.gwu.edu> .

[37] K. Hagiwara *et al.* [Particle Data Group Collaboration],

Phys. Rev. D **66**, 010001 (2002).